



PCCP

Detailed electronic structure of a high-spin cobalt(II) complex determined from NMR and THz-EPR spectroscopy

Journal:	<i>Physical Chemistry Chemical Physics</i>
Manuscript ID	CP-COM-03-2019-001474.R1
Article Type:	Communication
Date Submitted by the Author:	29-Mar-2019
Complete List of Authors:	Pavlov, Alexander; Nesmeyanov Institute of Organoelement Compounds of the Russian Academy of Sciences, Nehrkorn, Joscha; Max-Planck-Institut für chemische Energiekonversion, Pankratova, Yanina; INEOS RAN Ozerov, Mykhaylo; Florida State University, National High Magnetic Field Laboratory Mikhalyova, Elena; Pisarzhevskii Institute of Physical Chemistry, Polezhaev, Alexander; INEOS RAN Nelyubina, Yulia; A. N. Nesmeyanov Institute of Organoelement Compounds, Russian Academy of Sciences, X-ray diffraction center Novikov, Valentin; Nesmeyanov Institute of organoelement compounds, Russian Academy of Sciences,

SCHOLARONE™
Manuscripts

COMMUNICATION

Detailed electronic structure of a high-spin cobalt(II) complex determined from NMR and THz-EPR spectroscopy

Received 00th January 20xx,
Accepted 00th January 20xx

Alexander A. Pavlov,^{a,b*} Joscha Nehr Korn,^{c,d} Yanina A. Pankratova,^{a,e} Mykhaylo Ozerov,^c Elena A. Mikhalyova,^f Alexander V. Polezhaev,^a Yulia V. Nelyubina,^{a,b} and Valentin V. Novikov^{a,b}

DOI: 10.1039/x0xx00000x

Here we report a combined use of THz-EPR and NMR spectroscopy for obtaining a detailed electronic structure of a long-known high-spin complex, cobalt(II) bis[tris(pyrazolyl)borate]. The lowest inter-Kramers transition was directly measured by THz-EPR spectroscopy, while the energies of higher Kramers doublets were estimated by a recently proposed NMR-based approach. Together, they produced magnetic parameters for a full model that explicitly includes spin-orbit coupling. This approach is applicable to all transition metal ions for which the spin-orbit coupling cannot be treated perturbatively.

Getting insight into fine details of electronic structure is crucial for rational design of new magnetic materials based on transition metal complexes, such as single molecule magnets¹⁻⁴ and spin-crossover compounds⁵⁻⁷ in molecular spintronics^{8,9} or paramagnetic tags in structural biology¹⁰⁻¹². Many methods exist to probe the electronic structure of their ground term, which governs the magnetic properties of these materials. In addition to commonly employed techniques, such as optical absorption and fluorescence spectroscopy^{13,14}, EPR spectroscopy¹⁵, magnetometry^{16,17} and X-ray diffraction¹⁸, other approaches are being developed. Among them, Frequency-Domain Fourier-Transform THz electron paramagnetic resonance spectroscopy (THz-EPR) directly probes transitions within an exceptionally broad excitation range (up to hundreds cm^{-1}), far beyond the range of routine EPR spectrometers^{19,20}. Although it provides unique

information on the electronic structure of transition metal complexes, accessing higher lying excited states is still a challenge due to the selection rules and low temperatures usually employed in these measurements to obtain better signal-to-noise ratios. Therefore, a technique complimentary to THz-EPR spectroscopy is needed, such as, e.g., NMR spectroscopy. A popular tool for identifying diamagnetic compounds in solutions, it recently emerged as a powerful approach for probing the electronic structure of paramagnetic transition metal complexes at ambient temperatures²¹⁻²⁸. Nevertheless, neither THz-EPR nor paramagnetic NMR spectroscopy are routinely used for this purpose. Here, both of them are applied to obtain the detailed electronic structure of a high-spin (HS) cobalt(II) complex with a trigonal antiprismatic geometry, which, e.g., often accounts for single molecule magnet behaviour²⁹. A well-known example of such type of complexes is cobalt(II) bis[tris(pyrazolyl)borate] (**CoTp₂**), introduced by S. Trofimenko in 1966³⁰. Its electronic structure has already been probed by a variety of optical and magnetic resonance methods³¹⁻³⁵. They showed that strong spin-orbit coupling (SOC) split the ⁴T_{1g} ground term of the cobalt(II) ion in a trigonal antiprismatic D₃ environment into six Kramers doublets (KDs), and the four lowest KDs are almost equidistant in energy with a separation of 206–242 cm^{-1} (Fig. 1)³².

We collected the THz-EPR spectra (see SI for experimental details) of **CoTp₂** from its fine-crystalline sample at NHMFL (Tallahassee, FL). Subsequently constructed Magnetic Field Division spectra (MDS) have very sharp features that are rarely observed in these kind of spectra^{36,37}. In the obtained MDS (see ref. ¹⁹ for more details), a minimum appears at 197 cm^{-1} in the zero magnetic field (Fig. 2) together with maxima at lower and higher energies, respectively. Upon increasing the magnetic field, the former feature broadens, and the latter shifts to lower and higher energies, respectively. While the minimum and the low-energy maximum broaden beyond recognition at higher fields, the high-energy maximum is recognizable over the probed field range. No further magnetic signals could be detected.

^a A.N.Nesmeyanov Institute of Organoelement Compounds, Russian Academy of Sciences, Vavilova str. 28, 119991, Moscow, Russia. E-mail: pavlov@ineos.ac.ru

^b Moscow Institute of Physics and Technology, Institutskiy per., 9, Dolgoprudny, Moscow Region, 141701, Russian Federation

^c National High Magnetic Field Laboratory & Florida State University, 1800 E. Paul Dirac Drive, Tallahassee, FL 32310-3706, USA

^d Max Planck Institute for Chemical Energy Conversion, Stiftstr. 34–36, 45470 Mülheim an der Ruhr, Germany

^e Lomonosov Moscow State University, Leninskie Gory, Moscow, 119991, Russia.

^f L.V.Pisarzhetskii Institute of Physical Chemistry of the National Academy of Sciences of the Ukraine, Prospekt Nauki 31, Kiev, 03028, Ukraine

†Electronic Supplementary Information (ESI) available: experimental and calculation details as well as supplementary tables and figures. See DOI: 10.1039/x0xx00000x

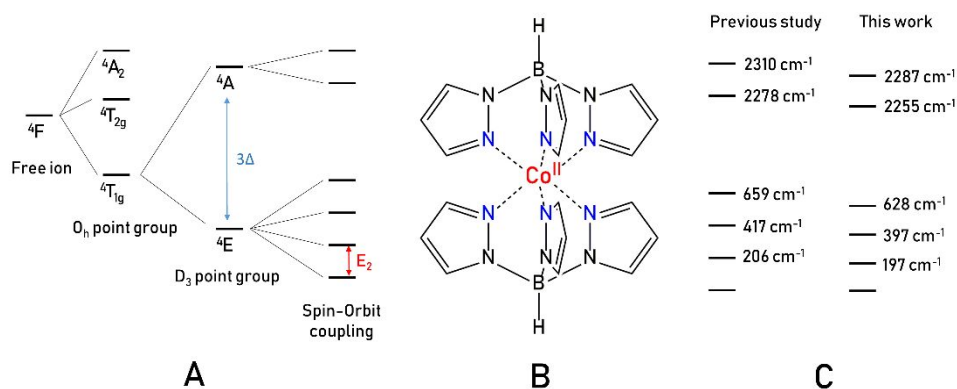


Figure 1. (A) Electronic structure of the high-spin cobalt(II) ion in a D_3 environment with significant spin-orbit coupling. Δ is a parameter of crystal field splitting of the ground term $^4T_{1g}$. (B) Cobalt(II) bis[tris(pyrazolyl)borate] CoTp_2 . (C) Energy levels in CoTp_2 according to the previous study³² and in this work.

The simulations of FD-FT THz-EPR MDS with an effective Spin-Hamiltonian (1), which has no rhombic terms due to the axial symmetry of CoTp_2 , gave us the magnitude of the zero-field splitting (ZFS) parameter $|D|$ of 98.5 cm^{-1} and $g_{\perp} = 1.9$, $g_{\parallel} = 2.1$.³⁸⁻⁴⁰

$$\hat{H} = D\left(\hat{S}_z^2 - \frac{S^2}{3}\right) + \mu_B \mathbf{B}_0 \cdot \text{diag}(g_{\perp}, g_{\perp}, g_{\parallel}) \cdot \hat{S} \quad (1)$$

Although the effective Spin Hamiltonian should not be, in fact, used for systems with low-lying orbital states,³² simulations with eq. 1 provided spectra that agree nicely with those measured experimentally (see Fig. 2), as they were measured at 4.2 K. At this temperature, only the 1st KD is significantly populated in CoTp_2 ; probabilities of transitions from the 1st KD

to the 3rd and higher lying KDs are hardly probable, so they cannot be accessed with THz-EPR spectroscopy. However, it might be still possible with techniques operating at higher temperatures, such as NMR spectroscopy. In an approach that we have recently proposed,^{21,22,41} the energy of the KDs are related to the molar magnetic susceptibility tensor anisotropy $\Delta\chi$, which can be obtained by the NMR spectroscopy:

$$\Delta\chi_{ax} = \chi_{\parallel} - \chi_{\perp} \quad (2)$$

$$\chi_a = \frac{N_A k T}{10} \frac{\partial^2}{\partial B_a^2} \ln \left(\sum_i e^{-\frac{(\psi_i | \hat{H} | \psi_i)}{kT}} \right) \quad (3)$$

where ψ_i are the eigenvectors of a spin-Hamiltonian; $a = \parallel, \perp$.

In the NMR spectra recorded from a solution of a paramagnetic compound (Figs S1-S3), this anisotropy $\Delta\chi$ causes a pseudocontact chemical shift of each nucleus, δ_{PCS} , according to where it is found related to the paramagnetic center in a molecule. In the case of an axial symmetry, such as in CoTp_2 :

$$\delta_{PCS} = \frac{1}{12\pi r^3} \Delta\chi_{ax} (3\cos^2\theta - 1) \quad (4)$$

Here, $\Delta\chi_{ax}$ is the axial anisotropy of the magnetic susceptibility tensor (χ -tensor), and r and θ are polar coordinates of a nucleus in the χ -tensor frame.

The other two components of the chemical shifts in the NMR spectra are of diamagnetic and contact origins. The diamagnetic contribution, which arises from the shielding of nuclei by the orbital motion of paired electrons, can easily be obtained by NMR spectroscopy of a diamagnetic analogue, such as an isostructural complex of a diamagnetic metal or a free ligand. The contact contribution δ_{CS} results from the delocalization of spin density ρ through a system of molecular orbitals and is, therefore, accessible by a simple quantum chemical calculation:

$$\delta_{CS} = \frac{4\pi\mu_B}{9kT} g^{iso} \rho \quad (5)$$

For CoTp_2 , the introduced approach (see SI for more details) allowed us to obtain chemical shifts in ^1H , ^{13}C and ^{11}B NMR spectra that were in a good agreement with those measured experimentally from its solution in toluene- d_8 at 200 – 340 K (Figs S4-S12). The fit between the calculated and measured chemical shifts, which is at the core of this procedure, produced accurate values of the anisotropy $\Delta\chi_{ax}$ in the corresponding temperature range (Fig. 3). They were then simulated using various models.

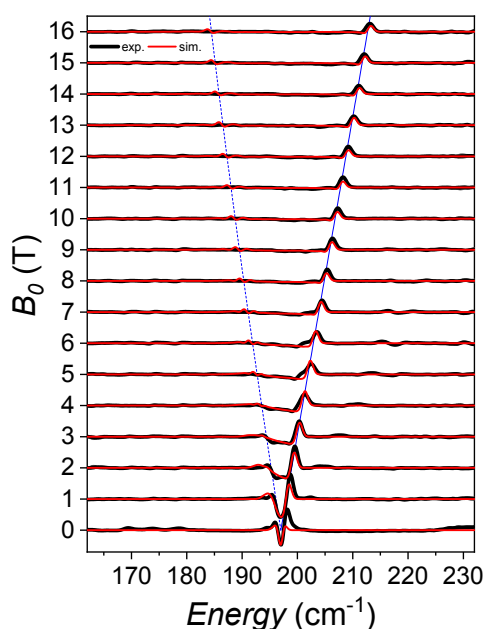


Figure 2. THz-EPR spectra for a fine-crystalline sample of CoTp_2 at 4.2 K (black). MDS spectra at the magnetic field B_0 are obtained by dividing a spectrum measured at $B_0 + 1 \text{ T}$; data is offset for B_0 . Simulation with the spin-Hamiltonian (1) ($S = 3/2$, $D = -98.5 \text{ cm}^{-1}$, $g_{\perp} = 1.9$, $g_{\parallel} = 2.1$) is shown in red. Blue lines correspond to the transition energies for B_0 perpendicular (dashed) and parallel (solid) to the molecular easy axis.

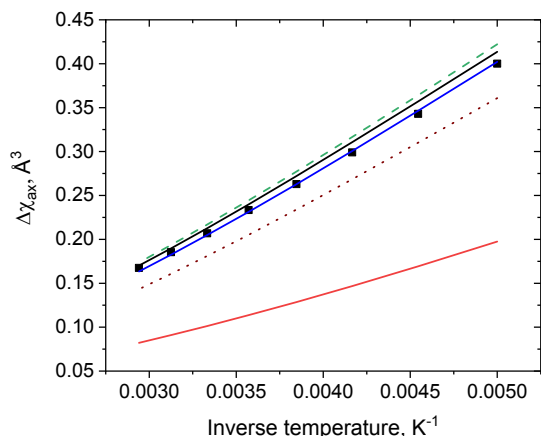


Figure 3. Temperature dependence of the magnetic susceptibility tensor anisotropy $\Delta\chi_{ax}$ for a solution of CoTp_2 in toluene- d_6 (black squares). Various simulations are included as lines. Simulations using Eq. 1 and $D = -98.5 \text{ cm}^{-1}$, $g_{\perp} = 1.9$, $g_{\parallel} = 2.1$ are shown as red solid line. Further simulations were done with Eq. 6. Simulation using the parameters ($\lambda = 152.4 \text{ cm}^{-1}$, $\sigma = 1.366$, $\Delta = -632 \text{ cm}^{-1}$) based on previous results³² are shown as black solid line. The best fit ($\lambda = 147.3 \text{ cm}^{-1}$, $\sigma = 1.350$ and $\Delta = -632 \text{ cm}^{-1}$) is shown as blue solid line. To visualize the sensitivity to Δ , we included simulations with fixed Δ values of -900 cm^{-1} (dashed green line) and -400 cm^{-1} (dotted brown line).

For most transition metal ions, the SOC can be treated as a perturbation leading to the ZFS formalism shown in Eq. 1⁴². An exception is HS Co(II) ion in a (distorted) octahedral or trigonal antiprismatic environment. To model the magnetic properties of CoTp_2 , SOC has to be explicitly included. If the common ${}^4\text{T}_{1g} \rightarrow {}^4\text{P}$ isomorphism is used,⁴³ an effective orbital angular momentum L is 1, and the Hamiltonian takes the following form:

$$\hat{H} = \sigma\lambda\hat{L} \cdot \hat{S} + \Delta(3\hat{L}_z^2 - \hat{L}^2) + \mu_B B_0(-\sigma\hat{L} + g_e\hat{S}) \quad (6)$$

Here, λ is the SOC parameter, σ is an orbital reduction factor and Δ parametrizes the crystal field splitting of the ground term ${}^4\text{T}_{1g}$ (Fig. 1), g_e is the free electron g -factor. A known limitation of this model is the interdependency of the above magnetic parameters. Although it is regularly applied to fit magnetometry results, obtaining a unique set of parameters with it is quite challenging. Thus, additional methods are required for this purpose.

While the results from THz-EPR spectroscopy could also be described with the effective Spin Hamiltonian (Eq. 1), we failed to obtain reasonable convergence to the NMR data. Therefore, the more elaborate Hamiltonian given in Eq. 6 was used. In the fitting routine, the zero-field energy difference between the first and second KD (E_2) was fixed to the spectroscopic value of 197 cm^{-1} . The resulting values $\lambda = 147.3 \text{ cm}^{-1}$, $\sigma = 1.350$ and $\Delta = -632 \text{ cm}^{-1}$ allowed reproducing the experimental THz-EPR spectra (Fig. S13) and the magnetic susceptibility for a solution of CoTp_2 (Fig. S14). Parameters based on the previously published energy diagram³² ($\lambda = 152.4 \text{ cm}^{-1}$, $\sigma = 1.366$, $\Delta = -632 \text{ cm}^{-1}$) resulted in a slightly worse agreement with the NMR data (see Fig. 3) but the THz-EPR spectra were not reproduced at all (Fig. S15). Our results indicate that the prefactor $|\sigma\lambda|$ of the SOC is almost equal to E_2 . Numerical calculations (Fig. S17)

showed that this is the case for $|\Delta| \gg |\sigma\lambda|$, so that $|\Delta| > 3|\sigma\lambda|$ as obtained here is sufficient to reach this limit. It is reasonable to assume that THz-EPR spectroscopy is less sensitive to higher-lying levels than paramagnetic NMR spectroscopy. Therefore, the effective Spin Hamiltonian (eq. 1) could be applied for the former but not for the latter.

The combination of THz-EPR and paramagnetic NMR spectroscopies thus gave very accurate magnetic parameters and, as a result, a detailed picture of the energy splitting in the ${}^4\text{T}_{1g}$ state of the complex CoTp_2 (Table S1). Although here it was used for the HS Co(II) ion in a trigonal antiprismatic environment, this approach might be applicable to other complexes containing transition metal ions for which SOC have to be considered explicitly.

In conclusion, a detailed electronic structure is derived for the long-known cobalt(II) bis[tris(pyrazolyl)borate] by the direct observation of the lowest inter-Kramers transition in its THz-EPR spectra and by use of an NMR-based approach to obtaining the energies of higher lying KDs.

Such insights are essentially needed for all the paramagnetic ions with a significant contribution from SOC, including lanthanides and some transition metals. For them, the effective Spin Hamiltonian is no longer valid, and an appropriate Hamiltonian with individual SOC and crystal field terms have to be used. The methods to obtain its often elusive parameters by NMR spectroscopy are especially attractive, as such experiments are relatively fast and cheap and, therefore, allow for high-throughput assessing of new transition metal complexes as potential materials in molecular spintronics and structural biology.

Conflicts of interest

There are no conflicts to declare.

Acknowledgements

This study was financially supported by Russian Science Foundation (project №18-73-00113). THz-EPR experiments were performed at the National High Magnetic Field Laboratory, which is supported by National Science Foundation Cooperative Agreement No. DMR-1644779 and the State of Florida. Y.V.N. and E.A.M. acknowledge the Foundation Volkswagen Stiftung Trilateral Partnerships – Cooperation Projects between Scholars and Scientists from Ukraine, Russia and Germany, Ref. Number 90343. Chemical characterization was performed with the financial support from Ministry of Science and Higher Education of the Russian Federation using the equipment of the Center for Molecular Composition Studies of INEOS RAS.

Notes and references

- 1 R. Sessoli, D. Gatteschi, A. Caneschi and M. Novak, *Nature*, 1993, **365**, 141.

- 2 R. Sessoli and A. K. Powell, *Coordination Chemistry Reviews*, 2009, **253**, 2328-2341.
- 3 J. M. Frost, K. L. Harriman and M. Murugesu, *Chemical science*, 2016, **7**, 2470-2491.
- 4 M. Atanasov, D. Aravena, E. Suturina, E. Bill, D. Maganas and F. Neese, *Coordination Chemistry Reviews*, 2015, **289**, 177-214.
- 5 J. F. Létard, G. Chastanet, P. Guionneau and C. Desplanches, *Spin-Crossover Materials: Properties and Applications*, 2013, 475-506.
- 6 G. Molnár, S. Rat, L. Salmon, W. Nicolazzi and A. Bousseksou, *Advanced Materials*, 2018, **30**, 1703862.
- 7 K. S. Kumar and M. Ruben, *Coordination Chemistry Reviews*, 2017, **346**, 176-205.
- 8 R. E. Winpenny, *Angewandte Chemie International Edition*, 2008, **47**, 7992-7994.
- 9 L. Bogani and W. Wernsdorfer, in *Nanoscience And Technology: A Collection of Reviews from Nature Journals*, World Scientific 2010, pp. 194-201.
- 10 I. Bertini, C. Luchinat, G. Parigi and E. Ravera, *NMR of Paramagnetic Molecules: Applications to Metallobiomolecules and Models*, Elsevier 2016.
- 11 H. Yagi, K. B. Pilla, A. Maleckis, B. Graham, T. Huber and G. Otting, *Structure*, 2013, **21**, 883-890.
- 12 M. A. Hass and M. Ubbink, *Current opinion in structural biology*, 2014, **24**, 45-53.
- 13 S. L. Reddy, T. Endo and G. S. Reddy, in *Advanced Aspects of Spectroscopy*, InTech 2012.
- 14 Y. Chia and M. Tay, *Dalton Transactions*, 2014, **43**, 13159-13168.
- 15 B. Gilbert, ed. *Electron Paramagnetic Resonance: Volume 21*, Royal Society of Chemistry 2008.
- 16 D. N. Woodruff, R. E. Winpenny and R. A. Layfield, *Chemical reviews*, 2013, **113**, 5110-5148.
- 17 D. Gatteschi, R. Sessoli and J. Villain, *Molecular nanomagnets*, Oxford University Press on Demand 2006.
- 18 C. Gatti and P. Macchi, *Modern charge-density analysis*, Springer Science & Business Media 2012.
- 19 J. Nehr Korn, K. Holldack, R. Bittl and A. Schnegg, *Journal of Magnetic Resonance*, 2017, **280**, 10-19.
- 20 P. Neugebauer, D. Bloos, R. Marx, P. Lutz, M. Kern, D. Aguilà, J. Vaverka, O. Laguta, C. Dietrich and R. Clérac, *Physical Chemistry Chemical Physics*, 2018, **20**, 15528-15534.
- 21 A. A. Pavlov, G. L. Denisov, M. A. Kiskin, Y. V. Nelyubina and V. V. Novikov, *Inorganic chemistry*, 2017, **56**, 14759-14762.
- 22 V. V. Novikov, A. A. Pavlov, Y. V. Nelyubina, M.-E. Boulon, O. A. Varzatskii, Y. Z. Voloshin and R. E. Winpenny, *Journal of the American Chemical Society*, 2015, **137**, 9792-9795.
- 23 T. Morita, M. Damjanović, K. Katoh, Y. Kitagawa, N. Yasuda, Y. Lan, W. Wernsdorfer, B. K. Breedlove, M. Enders and M. Yamashita, *Journal of the American Chemical Society*, 2018, **140**, 2995-3007.
- 24 M. Hiller, S. Krieg, N. Ishikawa and M. Enders, *Inorganic chemistry*, 2017, **56**, 15285-15294.
- 25 M. Findeisen, T. Brand and S. Berger, *Magnetic Resonance in Chemistry*, 2007, **45**, 175-178.
- 26 M. Damjanovic, K. Katoh, M. Yamashita and M. Enders, *Journal of the American Chemical Society*, 2013, **135**, 14349-14358.
- 27 V. V. Novikov, A. A. Pavlov, A. S. Belov, A. V. Vologzhanina, A. Savitsky and Y. Z. Voloshin, *The journal of physical chemistry letters*, 2014, **5**, 3799-3803.
- 28 A. A. Pavlov, Y. V. Nelyubina, S. V. Kats, L. V. Penkova, N. N. Efimov, A. O. Dmitrienko, A. V. Vologzhanina, A. S. Belov, Y. Z. Voloshin and V. V. Novikov, *The journal of physical chemistry letters*, 2016, **7**, 4111-4116.
- 29 J. Zhang, J. Li, L. Yang, C. Yuan, Y.-Q. Zhang and Y. Song, *Inorganic chemistry*, 2018, **57**, 3903-3912.
- 30 S. Trofimenko, *Journal of the American Chemical Society*, 1966, **88**, 1842-1844.
- 31 S. Trofimenko, *Journal of the American Chemical Society*, 1967, **89**, 3170-3177.
- 32 J. Jesson, *The Journal of Chemical Physics*, 1966, **45**, 1049-1056.
- 33 J. Jesson, S. Trofimenko and D. Eaton, *Journal of the American Chemical Society*, 1967, **89**, 3148-3158.
- 34 D. L. Tierney, *The Journal of Physical Chemistry A*, 2012, **116**, 10959-10972.
- 35 A. R. Marts, J. C. Kaine, R. R. Baum, V. L. Clayton, J. R. Bennett, L. J. Cordonnier, R. McCarrick, A. Hasheminasab, L. A. Crandall and C. J. Ziegler, *Inorganic chemistry*, 2016, **56**, 618-626.
- 36 M. A. Palacios, J. Nehr Korn, E. A. Suturina, E. Ruiz, S. Gómez-Coca, K. Holldack, A. Schnegg, J. Krzystek, J. M. Moreno and E. Colacio, *Chemistry—A European Journal*, 2017, **23**, 11649-11661.
- 37 J. Nehr Korn, S. L. Veber, L. A. Zhukas, V. V. Novikov, Y. V. Nelyubina, Y. Z. Voloshin, K. Holldack, S. Stoll and A. Schnegg, *Inorganic chemistry*, 2018, **57**, 15330-15340.
- 38 S. Stoll and A. Schweiger, *Journal of magnetic resonance*, 2006, **178**, 42-55.
- 39 J. Nehr Korn, J. Telsler, K. Holldack, S. Stoll and A. Schnegg, *The Journal of Physical Chemistry B*, 2015, **119**, 13816-13824.
- 40 J. Nehr Korn, A. Schnegg, K. Holldack and S. Stoll, *Physical review letters*, 2015, **114**, 010801.
- 41 A. A. Pavlov, S. A. Savkina, A. S. Belov, Y. Z. Voloshin, Y. V. Nelyubina and V. V. Novikov, *ACS Omega*, 2018, **3**, 4941-4946.
- 42 A. Abragam and B. Bleaney, *Electron paramagnetic resonance of transition ions*, OUP Oxford 2012.
- 43 M. Lines, *The Journal of Chemical Physics*, 1971, **55**, 2977-2984.